The EMBO Journal Vol.18 No.6 pp.1689–1700, 1999

Self assembly of NuMA: multiarm oligomers as structural units of a nuclear lattice

Jens Harborth, Jian Wang, Catherine Gueth-Hallonet[1], Klaus Weber and Mary Osborn[2]

Department of Biochemistry, Max Planck Institute for Biophysical Chemistry, Am Fassberg 11, 37077 Goettingen, Germany

[1]Present address: Institut de Biologie Moleculaire des Plantes, 12 rue du General Zimmer, 67084 Strasbourg, France

[2]Corresponding author
e-mail: mosborn@gwdg.de

NuMA is a nuclear matrix protein in interphase and relocates to the spindle poles in mitotis. Different NuMA constructs, in which either N- or C-terminal domains were deleted, and the full-length construct were expressed in *Escherichia coli*, and the NuMA polypeptides were purified to homogeneity and allowed to assemble *in vitro*. Electron microscopy showed that NuMA can build multiarm oligomers by interaction of the C-terminal globular domains. Each arm of the oligomer corresponds to a NuMA dimer. Oligomers with up to 10 or 12 arms have been observed for both full-length NuMA and for constructs that still contain the proximal part of the C-terminal tail domain. Other results from this laboratory have shown that transient overexpression of NuMA in HeLa cells induces a nuclear scaffold with a quasi-hexagonal organization that can fill the nuclei. Here we show that computer modelling of the three-dimensional packing of NuMA into such scaffolds can explain the different spacing of the hexagons seen when constructs with different coiled-coil lengths are used. Thus, the 12 arm oligomer, for which we have *in vitro* evidence, may be the structural unit from which the nuclear scaffold in transfected cells is built.

Keywords: multiarm oligomer/nuclear matrix/nuclear scaffold/NuMA/self-assembly

Introduction

The nuclear mitotic apparatus protein (NuMA) was first identified by its striking cell cycle-dependent shuttling (Lydersen and Pettijohn, 1980). NuMA is a phosphoprotein and shuttling is controlled by defined phosphorylation/dephosphorylation steps (Compton and Luo, 1995; Sparks *et al.*, 1995). In interphase cells, NuMA is restricted to the nucleus, whereas in mitotic cells it localizes to the spindle poles. In interphase cells, NuMA is a component of the nuclear matrix as shown by the classic criteria of being insoluble after DNase and high salt treatment of the nucleus. It is also resistant to extraction by non-ionic detergents but it can be solubilized by high concentrations of urea (Lydersen and Pettijohn, 1980; Kallajoki *et al.*, 1991; Harborth *et al.*, 1995). In addition, DNA binding studies have shown that NuMA is found associated with certain matrix associated regions (MARs) *in vitro* (Luderus *et al.*, 1994). In mitotic cells, NuMA is a functional part of the mitotic spindle, since microinjection of certain NuMA antibodies causes cells to become blocked in mitosis and/or to form micronuclei (Kallajoki *et al.*, 1991, 1993; Yang and Snyder, 1992). More recently, NuMA was shown to be an essential component for the formation and maintenance of mitotic spindle poles, and to interact with the dynein–dynactin complex (Gaglio *et al.*, 1995, 1996; Merdes *et al.*, 1996).

To date, two studies support the idea that NuMA can form lattice-like structures when overexpressed in HeLa cells (Saredi *et al.*, 1996; Gueth-Hallonet *et al.*, 1998). Overexpression of a NuMA construct lacking the nuclear localization signal (NuMA–ΔNLS) results in cells that show a single large cytoplasmic aggregate when stained with NuMA antibodies. Electron microscopy of such cytoplasmic aggregates revealed that they are composed of 5-nm diameter filaments and 23-nm diameter cables. Aggregates purified by flow cytometry contain only NuMA and are composed of 5-nm filaments (Saredi *et al.*, 1996). Overexpression of full-length (FL) NuMA results in cells that accumulate NuMA in nuclei, as shown using immunofluorescence microscopy (Gueth-Hallonet *et al.*, 1996; Saredi *et al.*, 1996). Recent experiments from this laboratory show that quasi-hexagonal lattices can be detected in nuclei of cells overexpressing FL NuMA after extraction with non-ionic detergent. Electron-dense particles are present at the hexagon vertices and in optimal sections, 5–6 nm filaments are seen connecting the vertices. Using mutant NuMA constructs with insertions or deletions in the coiled-coil domain, we showed that the lattice spacing was increased in the insertion mutants and decreased in the deletion mutants. The lattices are decorated by antibodies to NuMA (Gueth-Hallonet *et al.*, 1998).

The *in vivo* experiments suggest that NuMA might be capable of self assembly and for this reason it seemed important to analyse the *in vitro* assembly of NuMA in more detail. Secondary structure prediction rules indicated that NuMA should have a very long α-helical domain (169 kDa) flanked by globular head and tail domains of 24 and 45 kDa, respectively (Figure 1) (Compton *et al.*, 1992; Yang *et al.*, 1992). Previously we have studied the molecular properties of recombinant NuMA purified from *Escherichia coli*. We used chemical crosslinking studies, circular dichroism spectra and electron microscopy to directly reveal the tripartite structure of NuMA. The central rod is 207 nm long and at least 90% α-helical. It reflects a double-stranded coiled-coil with the α-helices arranged parallel and in register. Under the *in vitro* conditions we used originally, recombinant NuMA purified from *E.coli* neither assembled into filaments nor formed

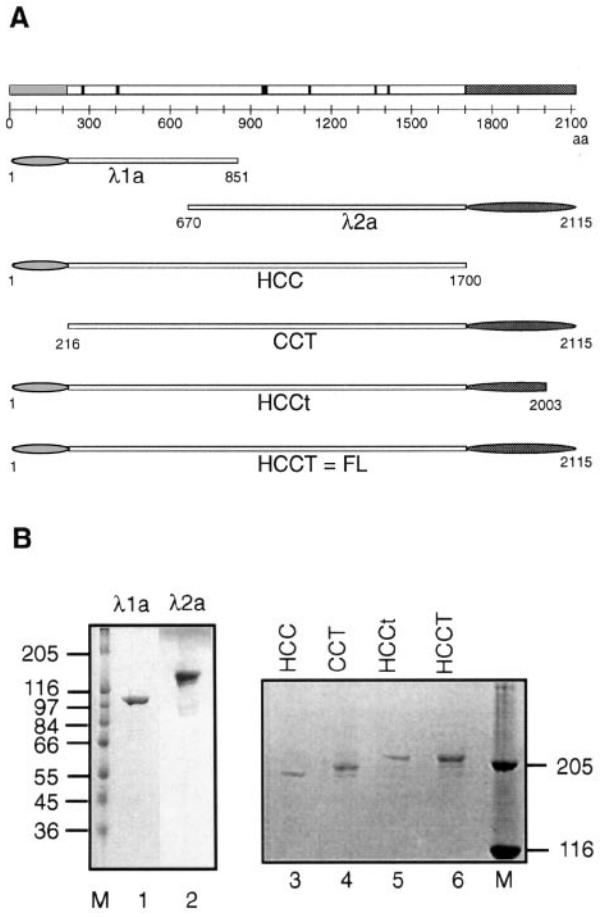

Fig. 1. (**A**) Secondary structure of the NuMA polypeptide proposed from the cDNA sequence. Note the long central α-helical region (unfilled region) consisting of seven helical subdomains interrupted by proline residues, flanked by globular head (grey shaded region) and (filled black region) tail domains. The relative positions of the recombinant clones, which are ligated in the pRSET expression vector and expressed as fusion proteins in *E.coli* are shown. (**B**) SDS–PAGE analysis of the purified recombinant NuMA constructs revealed apparent molecular masses in line with the sizes of 101 (lane 1), 167 (lane 2), 198 (lane 3), 218 (lane 4), 230 (lane 5) and 242 kDa (lane 6) predicted for these constructs (lanes 1 and 2, 10% SDS–PAGE; lanes 3–6, 5% SDS–PAGE). The constructs are designated according to the domains of the NuMA molecule they contain. H, head; CC, coiled-coil; T, tail; t, proximal part of tail. HCCT therefore corresponds to FL NuMA. M, molecular mass standards (numbers indicate $M_r \times 10^3$).

higher order structures, but was visualized using the electron microscope after rotary shadowing as dumbbell-shaped molecules corresponding to dimers (Harborth *et al.*, 1995).

Here we show that the previously reported formation of dimers by coiled-coil interactions is only the first step in oligomerization. By varying the conditions used for self assembly we now describe the formation of a novel structure, the multiarm oligomer. Each multiarm oligomer is formed by association of up to 12 NuMA dimers via their C-terminal domains. Multiarm oligomers are formed by both full-length NuMA and with certain derivatives that retain the proximal part of the tail domain. They are not seen when other constructs that do not contain this part of the NuMA molecule are used. In addition, computer modelling has been used to build models which use the 12 arm oligomer as the construction unit and which result in structures that appear very similar to the nuclear scaffolds seen in electron micrographs of cells transiently transfected with NuMA cDNAs. The fact that NuMA can self assemble into multiarm oligomers *in vitro* and can build three-dimensional lattices *in vivo* suggests that NuMA may serve a structural function in the interphase nucleus.

Results

Electron microscopy of the C-terminal λ 2a fragment shows multiarm oligomers

We first purified recombinant protein from the λ2a construct. This construct covers amino acid residues 670–2115 corresponding to the C-terminal 70% of the coiled-coil region and the entire globular tail domain (Figure 1A). The λ2a construct was cloned into the expression vector pRSET (Invitrogen) and expressed in *E.coli* JM109. After induction with IPTG, SDS–PAGE showed a major band of ~170 kDa (Figure 1B), in line with the expected size of this fragment. This band reacted on immunoblots with the NuMA monoclonal antibody SPN7 which detects an epitope between residues 1613 and 1700, i.e. at the end of the coiled-coil region (Harborth *et al.*, 1995). As the λ2a fragment was completely insoluble in lysis buffer, it was solubilized with 8 M urea and purified under denaturing conditions.

After dialysis against a 20 mM Tris buffer pH 7.2, containing 20 mM NaCl, the protein sample was glycerol sprayed, metal shadowed and examined using the electron microscope. The purified C-terminal λ2a construct revealed a novel oligomeric structure composed of a central core from which thin radial arms project in a multiarm array (Figure 2A). Each arm has the appearance expected for a single NuMA dimer. The multiarm oligomers contain different numbers of arms. The higher the number of arms the greater the size of the central core. We have observed oligomers composed of up to 12 dimers, although it is sometimes hard to distinguish the different rods and usually the oligomers have a lower number of arms (six to nine). The arms have an average length of 155 ± 15 nm. This is in good agreement with a value of 153 nm calculated for the length of the λ2a coiled-coil, assuming a value of 0.1485 nm per coiled-coil residue. The arms seem able to adopt different conformations, suggesting that they are flexible, and sometimes show a sharp bend at a position 110 nm from the central core (arrow in Figure 2A). This is a position that would be equivalent to the approximate centre of the coiled-coil region in the FL NuMA molecule.

Electron microscopy of the N-terminal fragment λ 1a reveals no oligomers

The N-terminal fragment λ1a, corresponding to amino acid residues 1–851, covers the entire head domain and the N-terminal 43% of the rod domain (Figure 1A). SDS–PAGE of the purified λ1a fragment showed a band of ~100 kDa (Figure 1B) that reacted in immunoblots with the SPN-3 antibody which recognizes an epitope located between residues 255 and 267 (Harborth *et al.*, 1995). The soluble protein was isolated by metal chelate chromatography on a Ni-NTA column and in a second step by gel filtration on a Superdex 200 column.

Oligomers were not found when this N-terminal frag-

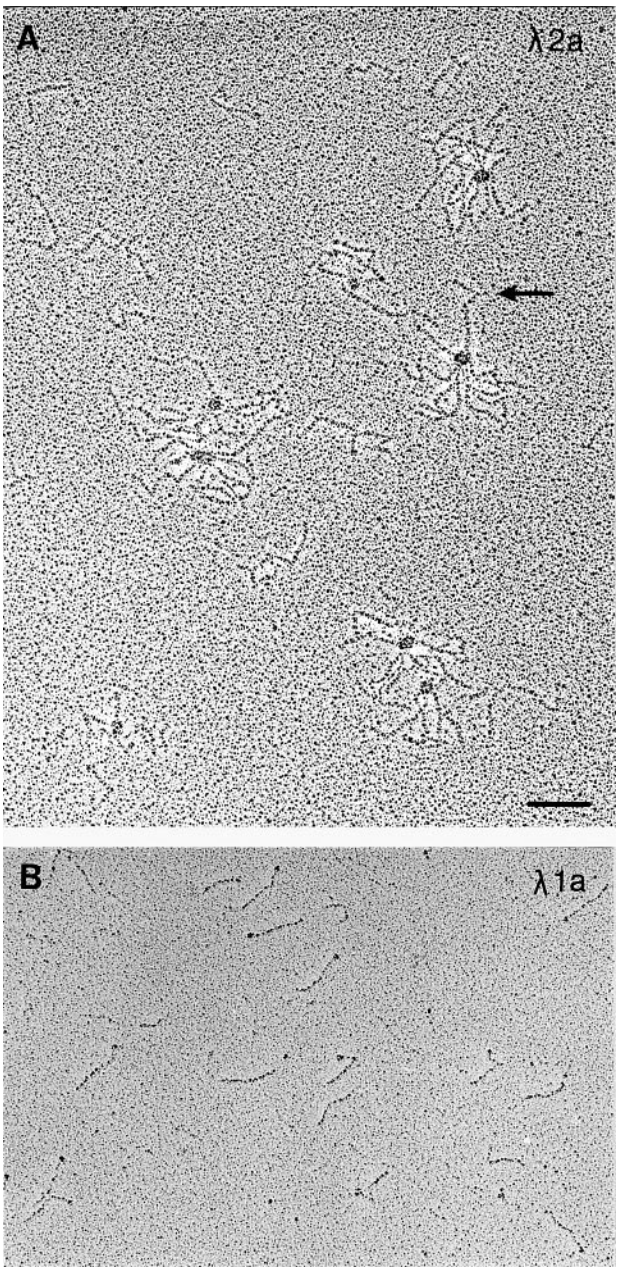

Fig. 2. Electron micrographs of purified recombinant NuMA fragments obtained after low angle rotary shadowing. (**A**) λ2a C-terminal fragment. Note the multiarm oligomers composed of a central globular core from which different numbers of arms project, and the sharp bends seen in some arms (arrow). (**B**) λla N-terminal fragment. Note the thin rods of uniform length with a globular head at one end and the lack of higher order oligomers. Bar represents 100 nm.

ment was examined using the electron microscope (Figure 2B). It shows only single rods with a small globule corresponding to the head at one end.

Location of C-termini to the centre of the multiarm oligomers using different NuMA mutants

The λ2a construct containing the C-terminal tail domain, but not the λ1a construct containing the N-terminal head domain, revealed multiarm oligomers. This suggested that the different NuMA dimers interact via the globular tail domains to form the multiarm oligomers. To obtain more evidence for this mode of assembly, we constructed

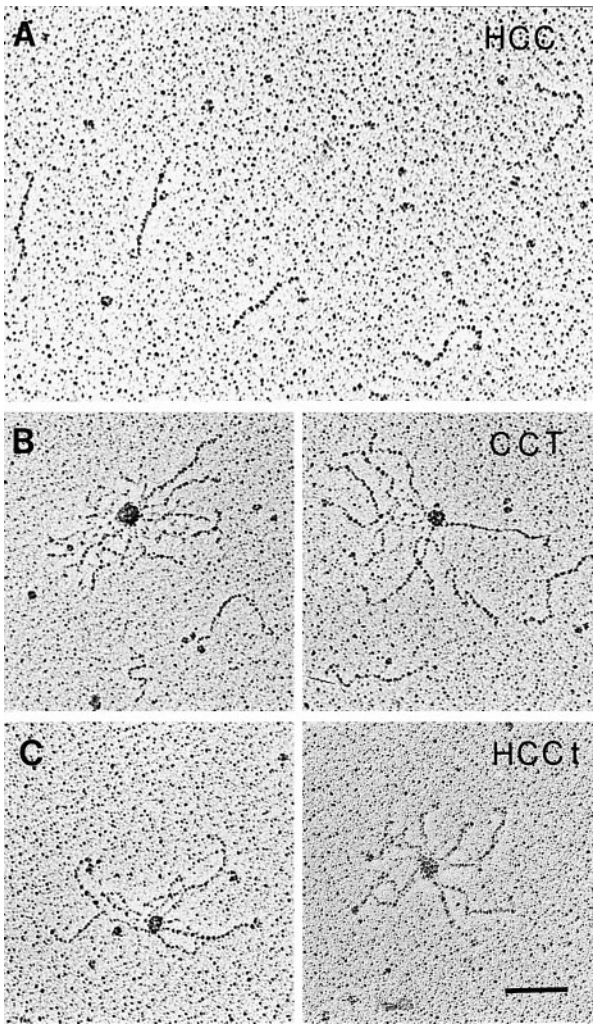

Fig. 3. Electron micrographs of recombinant NuMA fragments obtained after dialysis against physiological salt buffer and rotary shadowing. (**A**) HCC fragment, (**B**) CCT fragment and (**C**) HCCt fragment. Note that fragments with either the whole tail (CCT) or the proximal part of the tail (HCCt) show the multiarm oligomers whereas the fragment lacking the whole tail domain (HCC) shows only dimers. Globular structures are visible at the ends of the rods furthest from the centre for the HCCt fragment (C) but not for the headless mutant CCT (B). A globular structure is also visible at one end of some dimers formed from the HCC fragment (A). Bar represents 100 nm.

different mutants in which either the head or the tail domain was deleted. The constructs were designated according to the different patterns of the tripartite secondary structure they contain (see Materials and methods). These constructs were expressed in the pRSET vector in *E.coli* JM 109. Expression of such constructs was relatively low due to the very large size of the resulting fusion proteins. Only a small part of the tailless fragment (HCC residues 1–1700) was soluble in lysis buffer A. The construct containing a part of the tail domain (HCCt corresponding to residues 1–2003) was completely insoluble in this buffer, as were the complete recombinant protein (HCCT equivalent to full-length) and the construct without the N-terminal head domain (CCT corresponding to residues 216–2115). All four recombinant proteins (HCC, CCT, HCCt and HCCT) were purified by treating the insoluble pellets with 8 M urea to solubilize the recombinant protein. The fragments as well as the FL

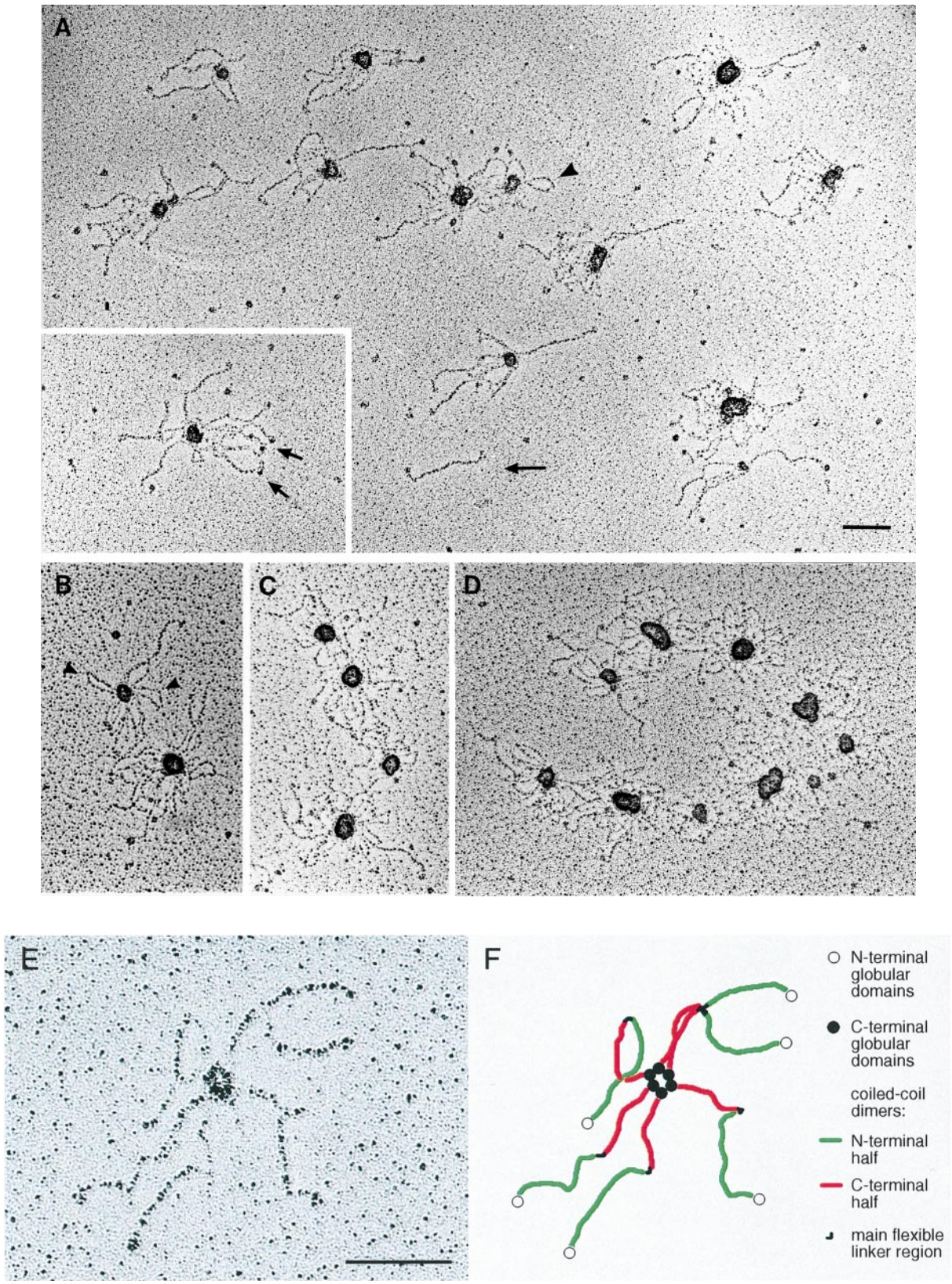

Fig. 4. Electron micrographs of the recombinant FL NuMA construct (HCCT) after renaturation from 8 M urea and rotary shadowing. (**A**) Overview to show the multiarm oligomers with a central globular core from which different numbers of arms project. Each arm is thought to represent a NuMA dimer. The size of the globular core increases as the number of arms increases. Globular head domains can be seen at the distal end of the arms (short arrows). In some oligomers individual arms show loops, which can be explained by bending of the coiled-coil domain. Sometimes the globular head domain binds to the globular tail domains in the central core (arrowhead). Note the single rod-shaped dimer molecule visible in (A) (long arrow). (B–D) Oligomers appear to be connected. In (**B**), FL NuMA was dialysed against 20 mM Tris pH 7.2, 150 mM NaCl, 1 mM EGTA, 1 mM DTT, 1 mM phenylmethylsufonylfluoride (PMSF). In (**C**) and (**D**), NuMA was dialysed against the same buffer with 20 mM NaCl. (**E** and **F**) Micrograph of a six arm oligomer (E) with sketch to show the arrangement of the individual dimers (F). Bar represents 100 nm.

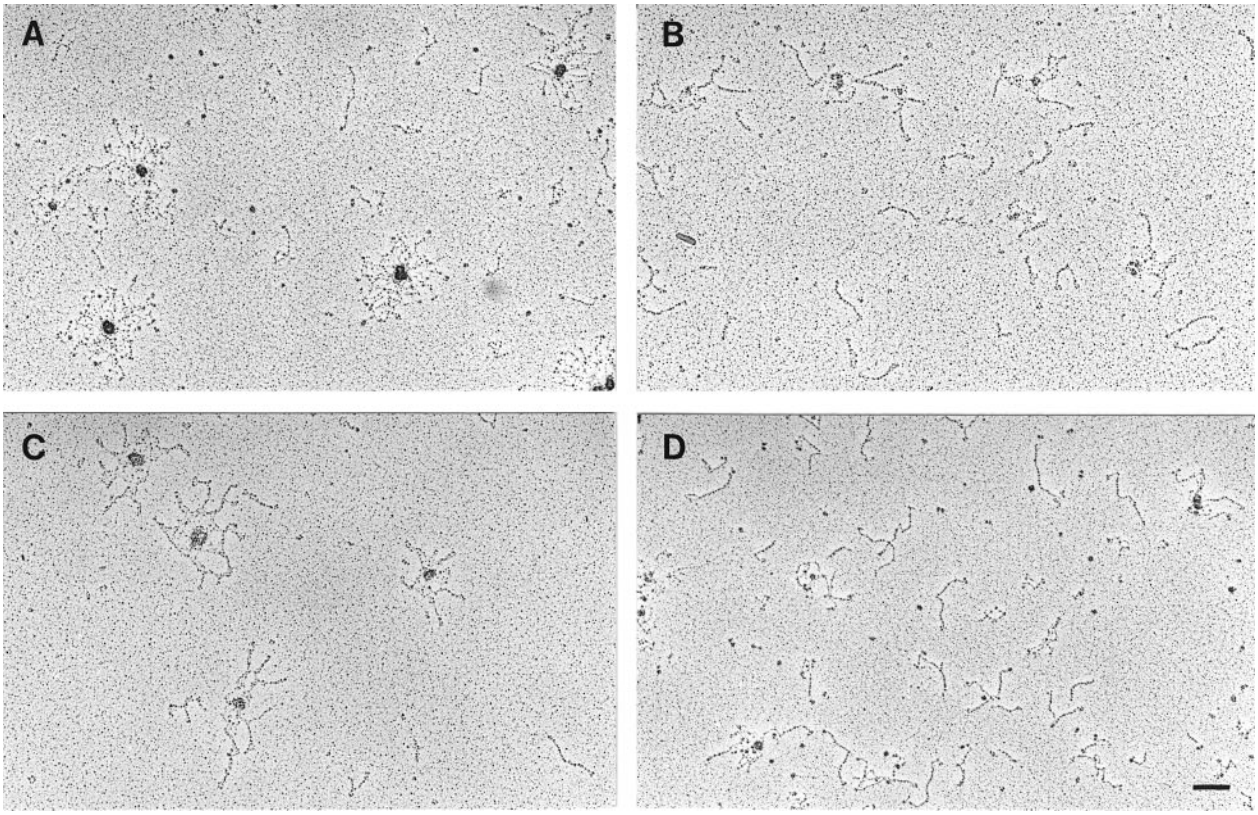

Fig. 5. Electron micrographs of recombinant FL NuMA. Purified protein was dialysed either against physiological salt buffer (**A**) or against high salt buffer (**B**). To show that the equilibrium is reversible, probes were also dialysed first against high salt buffer and then against physiological buffer (**C**) or first against physiological buffer and then against high salt buffer (**D**). Note that multiarm oligomers are visible in the samples dialysed against physiological salt buffer and that dimers are the predominant structure in the samples dialysed against high salt buffer. Bar represents 100 nm.

protein were purified in 8 M urea using a gel filtration column (TSK G6000 PW) as the first step. The recombinant proteins eluting in the first fractions absorbing UV light were pooled and applied to a MonoQ anion exchange column equilibrated with buffer in 8 M urea. The recombinant proteins were eluted using a salt gradient from 0 to 0.9 M NaCl. All four recombinant fragments eluted at a concentration of ~150 mM NaCl. Homogeneity was controlled by SDS–PAGE (Figure 1B). Before rotary shadowing, the proteins were renatured by dialysis against buffer D which does not contain urea. The resulting solutions of HCC, CCT, HCCt and HCCT were analysed by electron microscopy after glycerol spraying and metal shadowing (Figure 3). The tailless mutant (HCC) revealed only thin rods with globular portions at one end representing dimers (Figure 3A), whereas the headless mutant containing the full tail domain (CCT) clearly showed multiarm oligomers with a central core (Figure 3B). This result provides further evidence that FL NuMA interacts via the globular tail domains of the dimers. The construct HCCt, which contains only the proximal part of the tail domain, also showed clearly multiarm oligomers with a variable number of arms radiating from a central core (Figure 3C). This demonstrates further that the interaction, while requiring the proximal part of the tail domain, does not depend on the last 112 amino acid residues which are extremely basic (theoretical pI = 12.6). In addition, small globular structures corresponding to the head domain are visible at the end of the arms furthest from the central core in the multiarm oligomers formed from the HCCt mutant (Figure 3C), but not in those formed from the CCT construct (Figure 3B).

All three recombinant constructs (HCC, CCT and HCCt) have the complete α-helical domain, and indeed the rod-shaped portions of the different fragments have similar lengths of ~200 nm as shown in Figure 3. The rods seem able to bend, in agreement with our previous electron microscopic studies of recombinant FL NuMA which suggested that the rod regions of the molecule are flexible and that some were sharply bent at a hinge-like region near the middle of the molecule (Figure 8 in Harborth *et al.*, 1995).

Electron microscopy of the FL NuMA protein also reveals the multiarm oligomers

The results shown in Figures 2A and 3 caused us to investigate in more detail the *in vitro* assembly of the FL recombinant NuMA protein (residues 1–2115). Previously we presented a gallery of individual FL NuMA molecules that had an appearance similar to the molecule indicated with the long arrow in Figure 4A. In our previous experiments, which were performed at low protein concentrations (<0.02 mg/ml) or at high salt concentrations (500 mM NaCl), we saw only thin rods with globular heads and tails that correspond to NuMA dimers (Harborth *et al.*, 1995).

The FL construct was solubilized in 8 M urea, purified to homogeneity by gel filtration and anion exchange

chromatography, and renatured by dialysis as in previous experiments. In the experiments reported here, we used higher protein concentrations (>0.02 mg/ml) and different buffer conditions (physiological salt concentrations ≤150 mM), and under these conditions multiarm oligomers are the predominant form seen after renaturation of the FL NuMA molecules. Figure 4A shows an overview of the multiarm oligomers formed by renaturation of the FL construct into Tris-buffered saline (150 mM NaCl pH 7.2) at a concentration of 0.1 mg/ml. The multiarm oligomers have a globular core. The core diameter was again dependent on the number of arms, i.e. the higher the number of arms, the larger the core diameter. The arms were longer than those formed from the λ2a fragment (Figure 2A) and had an average length of 200 nm. This length is again in good agreement with the value of 221 nm calculated from the number of residues in the coiled-coil domain, and with a value of 207 nm measured from the length of the NuMA rod domain in the dimer. Each arm terminated at the outer extremity with a small globular domain that we showed in Figure 3 corresponded to the NuMA head domain (Figure 4A, arrows). Sometimes individual arms of the oligomers appeared as loops, suggesting that intramolecular interactions were occurring through backfolding of the globular head domain and interaction with the tail domains in the oligomer core (arrowheads in Figure 4A and B). Figure 4E shows a micrograph of a six-arm oligomer, while in Figure 4F the arrangement of the dimers forming this oligomer is illustrated.

Oligomers that seem to be interconnected can be found in some micrographs when protein concentrations of ~0.25 mg/ml are used. Figure 4B shows two oligomers that appear to be connected, Figure 4C shows four oligomers that are linked and Figure 4D shows a string of 10 oligomers. The core domains have an average centre-to-centre spacing (or interparticle distance) of 173 ± 28 nm. The core domains in Figure 4B–D have an average diameter of 48 ± 8 nm.

The oligomerization of NuMA into multiarm structures is reversible

We next tested whether the oligomerization of dimeric NuMA molecules into multiarm structures via the C-terminal globular domain was reversible. We purified the FL construct under denaturing conditions in the presence of 8 M urea. The protein solution with a concentration of ~0.1 mg/ml was dialysed against either a physiological salt buffer containing 150 mM NaCl or a high salt buffer containing 500 mM NaCl. Samples were dialysed in parallel. Other samples were dialysed first against the high salt buffer and then against the physiological salt buffer or vice versa (Figure 5). FL NuMA clearly showed the multiarm oligomers when dialysed against a buffer containing 150 mM NaCl (Figure 5A) as expected from the results in Figure 3, whereas in the presence of 500 mM NaCl only dumbbell molecules corresponding to dimers were seen (Figure 5B). Samples first dialysed against the high salt buffer and then against the physiological salt buffer built multiarm oligomers from the dimer molecules (Figure 5C) showing a reversible transition from the dimer state to the multiarm oligomer. Conversely, multiarm oligomers built in the physiological salt buffer dissociated to dimers when dialysed subsequently against the high salt buffer (Figure 5D), showing a reversible transition from the multiarm oligomer to the dimer.

Lattices in nuclei of HeLa cells overexpressing FL NuMA

Examples of the type of lattices that can be seen in HeLa cells overexpressing FL NuMA or different NuMA constructs are shown in Figure 6. The cells have been incubated for 42 h after transfection and then extracted with a microtubule stabilizing buffer containing 0.5% Triton X-100. They were fixed in glutaraldehyde and embedded as monolayers for electron microscopy. Figure 6 compares and contrasts the profiles obtained from normal control cells (Figure 6A) and from cells transfected with either the FL construct (Figure 6B and F) or with constructs with insertions or deletions in the coiled-coil region (Figure 6C–E and G–I). In normal untransfected cells, only residual patches of chromatin and residual proteinaceous structures are retained (Figure 6A). In cells transfected with the FL construct, a striking network that fills the nucleoplasm can be discerned. At higher magnification this structure appeared to be formed from a three-dimensional network of hexagons with electron dense particles at each vertex and at the centre of the hexagon (Figure 6F). Different constructs with in-phase deletions or an in-phase insertion in the coiled-coil region change the spacing of the lattices (Figure 6C–E and G–I). The spacing of the hexagons measured for each of the different constructs from the electron micrographs is listed in the last column of Table I and is taken from Gueth-Hallonet *et al.* (1998). Overexpression of NuMA constructs with deletions in the coiled-coil domain (i.e. dCC1 and dCC2) yield hexagons with the spacing decreased by 19 or 39% in comparison with FL NuMA. In contrast, a construct with an in-frame insertion (CCXL) shows hexagons with the spacing increased by 42% in comparison to FL NuMA.

Computer modelling and discussion

Computer modelling of nuclear lattices using the 12 arm oligomer as structural unit

Ball-and-stick models using the 12 arm oligomer as the structural unit can explain the hexagonal organization seen in the electron micrographs. The model in Figure 7A uses hexagonal closest packing while the model in Figure 7B uses cubic closest packing. Computer modelling suggests that planar hexagonal arrangements of the type visualized in the electron micrographs of the FL NuMA construct (Figure 6B and F), i.e. with a central particle surrounded by six further particles, can be generated from both models by taking a slice either in the plane of the paper or by taking slices through the model at different angles. Patterns with a quadratic arrangement of particles have also been visualized in the lattices *in situ* and can be generated from the computer models.

Two possible arrangements of the NuMA dimers in a single lattice plane are shown in Figure 7C. In the first step of assembly, dimers are formed by aggregation of two monomers with the α-helices arranged parallel and in register (Figure 7C, top centre). In the second step of assembly, the globular C-terminal regions, indicated by a

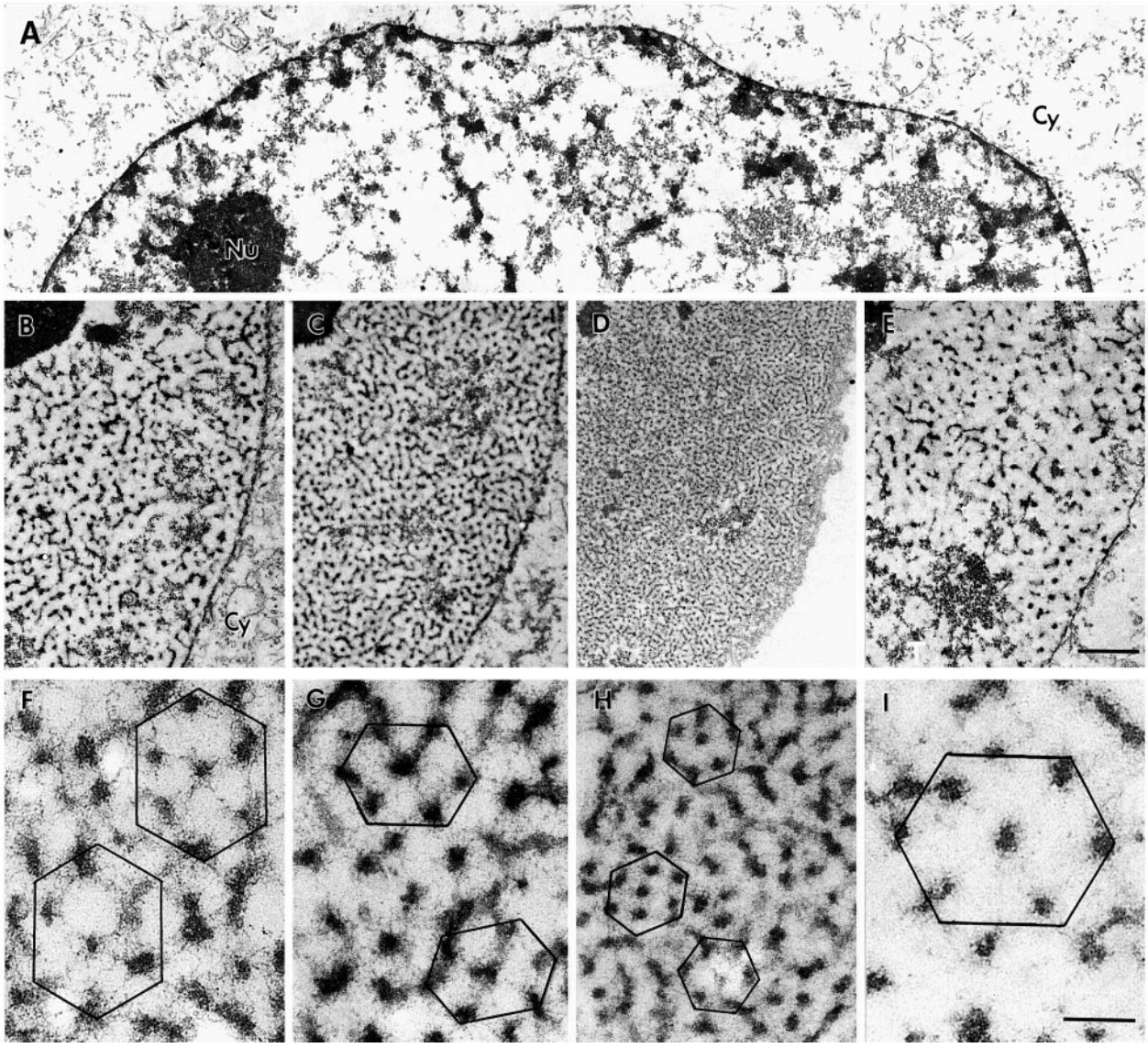

Fig. 6. Electron microscopy after detergent extraction of HeLa cells 42 h after transfection. (**A**) Mock transfected cell; (**B** and **F**) cells transfected with FL NuMA; (**C** and **G**) dCC1; (**D** and **H**) dCC2; or (**E** and **I**) CCXL NuMA cDNAs. The relative lengths of the coiled-coils in the different constructs in arbitrary units are dCC2 (0.4)<dCC1 (0.6)<FL (1.0)<CCXL (1.8). Note the ordered lattices that fill the nuclei in cells transfected with NuMA cDNAs (B–I). Hexagons are marked and thin 5–6 nm rods connecting the hexagon vertices can be seen in the high-magnification micrographs in (F–I). The relative sizes of the hexagons for the different constructs are dCC2<dCC1<FL<CCXL (for exact values and comparison to calculated values see Table I). Bar (A–E), 1 μm; (F–I), 200 nm. Part of the nucleolus is visible in (A) and at top left of B–E. Cy, cytoplasm; Nu, nucleolus.

Table I. Comparison of calculated values using models 1 and 2 with the measured centre-to-centre distance for the different constructs

	Total no. residues[a]	Coiled-coil residues[a]	Calculated rod length[b]	Measured particle diameter[c]	Centre-to-centre distance, no bending[d]	Centre-to-centre distance with bending[e]	Measured centre-to-centre distance[c]
FL	2115	1485	221	58	279	169	166 ± 14
CCXL	3327	2699	401	65	466	266	236 ± 27
dCC1	1523	894	133	44	177	111	135 ± 20
dCC2	1244	615	91	41	132	87	102 ± 13
Δ2005	2005	1485	221	26	247	137	130 ± 10

[a]Values from Yang *et al.* (1992).
[b]Calculated using a value of 0.1485 nm per coiled-coil residue (Harborth *et al.*, 1995).
[c]Taken from Gueth-Hallonet *et al.* (1998).
[d]Calculated by adding the particle diameter to the calculated coiled-coil length (model 1, Figure 7C in which the coiled-coils do not bend).
[e]Calculated by adding the particle diameter to half the coiled-coil length (model 2, Figure 7C in which the rod bends to achieve maximum packing of NuMA).

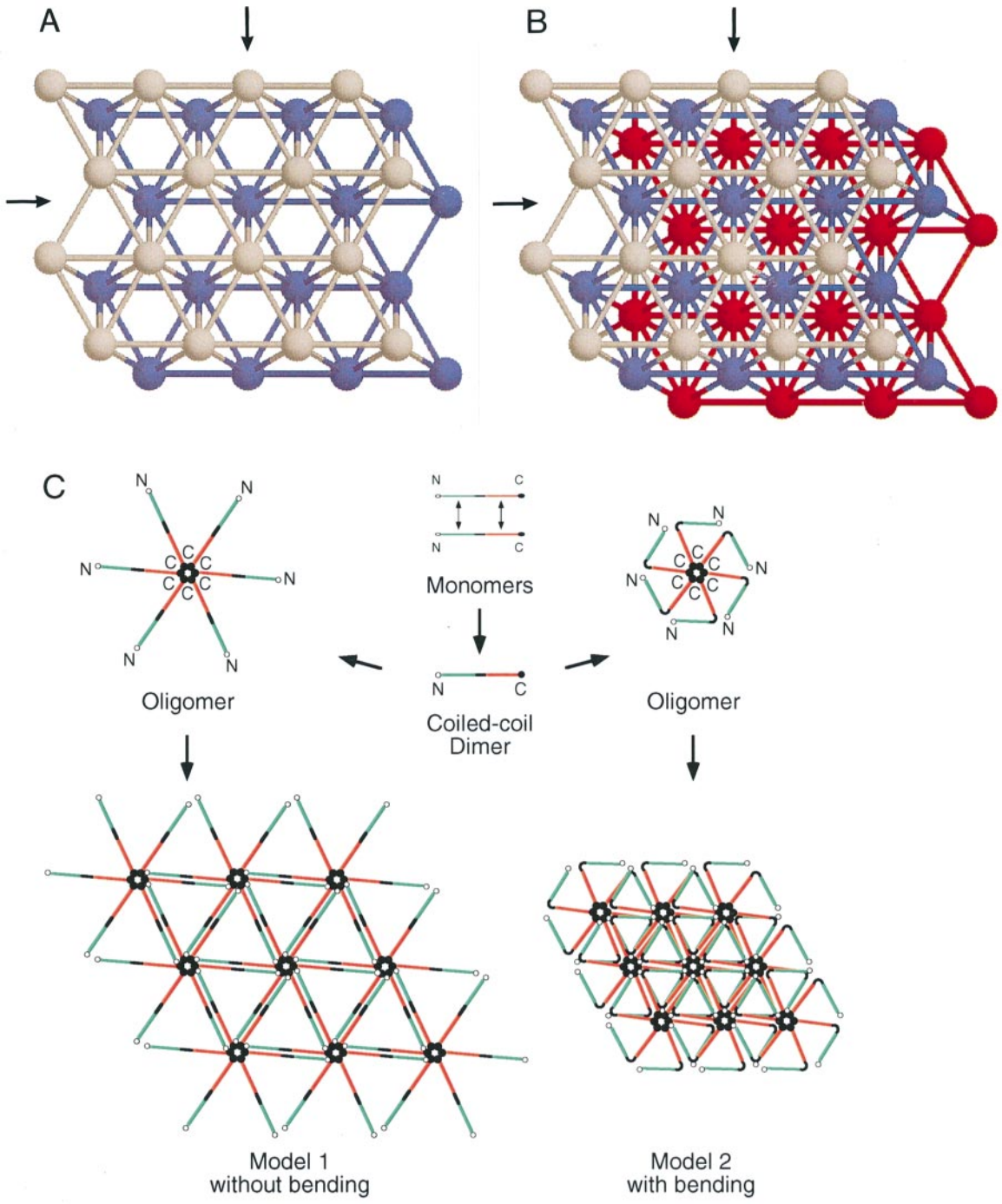

Fig. 7. (**A** and **B**) Three-dimensional ball-and-stick models of close packing of NuMA molecules in cells transfected with the FL construct. The balls represent the electron dense regions at the vertices of the quasi-hexagonal lattices while the sticks joining the balls represent the coiled-coil regions visualized as thin rods in the electon micrographs. In both models, each ball is surrounded by 12 nearest neighbours: six are in the planar hexagonal array, three are in the layer above and three are in the layer below. Each layer is drawn in the plane of the paper in a different colour; the difference in the models is best appreciated by focussing on the blue ball at the intersection of the arrows. (A) Hexagonal closest packing: the balls in the third layer lie over the balls in the first layer (pattern ABAB). (B) Cubic closest packing: the balls in the third layer lie over the grooves in the A layer (pattern ABCA). The balls represent oligomers of the NuMA globular domains. The sticks represent the coiled-coil portions of the NuMA molecules. (**C**) Models for the two-dimensional packing of NuMA in cells transfected with the FL construct. The formation of multiarm oligomers from dimers is illustrated in the top part of the figure. The dimers interact through their C-terminal globular domains (black dots). The globular head domains (black rings) can bind to the centres of neighbouring oligomers to form lattices in two and three dimensions, resulting in an anti-parallel array of the coiled-coil rods. The N-terminal half of the coiled-coil region is in green, the C-terminal half in red and the main bending region in the middle of the coiled-coil in black. A single line connecting the oligomers is used to represent each NuMA dimer. In model 1, the coiled-coil is not bent and the distance between the two centres corresponds to the coiled-coil length plus the particle diameter. In model 2, the coiled-coil is bent and the distance between two centres corresponds to half the coiled-coil length plus the particle diameter. In model 1, two dimers or four NuMA polypeptides connect the centres while in model 2 each centre is connected by four half-dimers or eight half-NuMA polypeptides.

Table II. Calculation of NuMA molecules required to assemble a lattice that fills the nucleus using models 1 and 2

	Model 1 no bending	Model 2 bending
Centre-to-centre distance[a]	279	169
Centres fitting into the nucleus[b]	7×10^4	3×10^5
Number of NuMA molecules[c]	1.7×10^6	7.2×10^6
Connections	4.2×10^5	1.8×10^6

[a]See Table I.
[b]Taking a value of 1000 μm^3 for the nucleoplasmic volume (given that in cross section, the nucleus of a typical HeLa cell approximates an ellipse with maximum dimensions of ~18.5×10.9 μm, we calculate a value for the nuclear volume of ~1150 μm^3, and then subtract 10% from this volume for the nucleolus).
[c]Calculated using 24 molecules per centre or 12 dimers per centre. These numbers can be compared with the number measured experimentally, i.e. 8×10^6 (see text).

black dot for each dimer, interact to form the globular centres. The experimental data described above show that the proximal part of the C-terminal domains are essential for formation of the multiarm oligomers and are found at the centre of such structures. The globular N-terminal regions, indicated by a black ring for each dimer, are shown interacting with the C-terminal regions and such interactions can be observed experimentally as shown in Figures 3 and 4. In the final assembly step, the multiarm oligomers aggregate to form a three-dimensional lattice. Experimental evidence for the existence of such lattices is provided by electron micrographs of HeLa cells which overexpress either FL NuMA or one of the constructs with additions or deletions in the coiled-coil (Figure 6; Gueth-Hallonet *et al*., 1998).

Models 1 and 2 in Figure 7C differ in the arrangement of the coiled-coils and as a consequence of this in the centre-to-centre spacing. In model 1, the coiled-coil is straight while in model 2 the coiled-coil region is bent approximately in the middle, corresponding to the bend sometimes seen in the middle of the coiled-coil (Figures 3 and 4). In model 1 the distance between the two centres corresponds therefore to the length of the coiled-coil plus the particle diameter, while in model 2 it corresponds to half the length of the coiled-coil plus the particle diameter. Model 1 therefore gives a larger centre-to-centre spacing (279 nm) than does model 2 (169 nm) (Table I). In addition, four times as many NuMA molecules can be packed into the nucleus using model 2 as with model 1 (Table II). Thus, in model 2, 7.2×10^6 molecules can be accommodated, whereas in model 1 only 1.7×10^6 molecules can be accommodated.

Comparison of models 1 and 2 with the experimental data for the FL construct and for constructs with changes in length of the coiled-coil region

The structural unit from which the models in Figure 7C are built is the 12 arm oligomer. The central core contains the C-terminal tail domains, and each arm corresponds to a single NuMA dimer. In Figures 2, 3 and 4 we provided experimental *in vitro* evidence for this structure and showed that its formation is dependent on the NuMA polypeptides retaining the proximal part of the C-terminal tail region.

How many polypeptides are found in the nucleus of a HeLa cell transfected with the FL NuMA construct? Such cells express 40 times more NuMA than do untransfected cells (Gueth-Hallonet *et al.*, 1996), while the abundance of NuMA in untransfected cells has been estimated at 2×10^5 polypeptides/cell (Compton *et al.*, 1992). This yields a value of 8×10^6 NuMA polypeptides per transfected cell, a value in good agreement with the value of 7.2×10^6 calculated using model 2 (Table II). This calculation also suggests that the number of NuMA molecules actually present in some transfected cells can exceed the number that can be packed into the nucleus. This may be why we find in one and the same cell not only a nuclear lattice, but also NuMA polypeptides accumulated in a single aggregate near to the centriole (Figure 6 in Gueth-Hallonet *et al*., 1998). In such cells it may be that the nucleus has become saturated with NuMA.

The calculated centre-to-centre spacings for models 1 and 2 can be compared directly with the measured centre-to-centre distances for the FL NuMA construct, and for the NuMA constructs with additions or deletions in the coiled-coil shown in Table I. The lengths for model 1, shown in column 6, were obtained by adding the calculated coiled-coil length to the measured particle diameter. The lengths for model 2, shown in column 7, were obtained by adding half the calculated length of the coiled-coil region to the measured particle diameter. The numbers in columns 6 and 7 can be compared directly with the measured centre-to-centre distances between particles in the hexagons observed in the electron microscope in column 8. The lengths predicted by model 1 are much larger than those actually observed, e.g. by a factor of 1.7 for the FL construct and 2.0 for the CCXL construct, and are greater than can be explained by shrinkage during the electron microscope procedures which can be ~10–20%. In contrast, the numbers provided by model 2 show a much better fit to the measured values e.g. a factor of 1.0 for the FL construct and 1.1 for the CCXL construct. Thus, model 2, which allows the coiled-coils to bend, again allows a better fit to the experimental data than does model 1, which shows the coiled-coil regions as stiff rods which cannot bend. The dCC1 and dCC2 constructs can also be accommodated in a model with bending (Table I).

Examination of the NuMA sequence shows the existence of six short non-helical spacers interrupting the sequence at different positions along the rod domain (6, 7, 19, 7, 5 and 6 amino acid residues in length) (Yang *et al.*, 1992). These non-helical spacers begin at residues 272, 401, 941, 1115, 1362 and 1410, respectively (see Figure 1A). More detailed analyses of the NuMA rod sequence have documented up to 13 additional discontinuities which do not involve prolines (Parry 1994). Circular dichroism results have provided direct experimental evidence that the NuMA rod is a segmented coiled-coil that does not reach 100% α-helix (Harborth *et al.*, 1995). Electron micrographs of isolated dimers (Figure 8 in Harborth *et al*., 1995) revealed a hinge-like region, probably corresponding to the major discontinuity beginning at residue 941 which is found approximately in the middle of the NuMA coiled-coil region. The results shown here in Figures 2, 3 and 4 confirm the existence of a major bending site and again

locate it to the middle of the coiled-coil region, but suggest that the FL molecule may also be able to bend at other positions along the molecule. Thus, the fact that the major bending site beginning at residue 941 has been deleted in the constructs dCC1 and dCC2 does not exclude that these constructs may also be able to bend. The position of the major bending site has been indicated in black in Figure 4F and in the models in Figure 7C.

NuMA assembly/disassembly: comparison of in vitro and in vivo data

Our data, together with the computer modelling data, suggest that the assembly of NuMA into lattices involves at least three steps: (i) dimer formation; (ii) formation of multiarm oligomers; and (iii) interaction of head and tail domains from different oligomers to form lattices. The first two steps occur by self assembly and require neither post-translational modifications nor additional proteins since they can be achieved starting from recombinant NuMA purified from *E.coli*. It may also be that step three occurs by self assembly. The fact that at protein concentrations of ~0.25 mg/ml some interconnected oligomers are seen (Figure 3B–D) provides a hint that this may be the case. However, it could be that post-translational modifications not provided by recombinant protein expression in *E.coli* may cause the oligomers to interact more efficiently and to build more stable three-dimensional lattices. Alternatively, specific kinases and/or phosphatases or other cofactors including binding proteins which are not present in our *in vitro* system might be required. The fact that NuMA assembles into higher order structures when a mitotic extract from HeLa cells is dephosphorylated (Saredi *et al.*, 1997) suggests that it may be possible to define further the factors required for lattice assembly using NuMA purified from the bacculovirus expression system and supplementing the assembly system with fractions from mitotic extracts that have been immunodepleted of NuMA.

Our *in vitro* data, as well as the models in Figure 7, suggest that deletions in the globular tail and head domains would have profound effects on lattice assembly, and indeed such effects have been noted in several experimental *in vivo* studies (Compton and Cleveland, 1993; Gueth-Hallonet *et al.*, 1998). The *in vitro* data show that the C-terminal globular domain is necessary to build the lattice structure since it is important for the first step in oligomerization. *In vivo* overexpression of certain NuMA constructs truncated in the tail domain, such as Δ2005, cause a drastic reorganization of nuclear components resulting in relocation of the DNA, histone H1 and nucleoli to the nuclear rim (see Figure 6 in Gueth-Hallonet *et al.*, 1998). The models suggest that deletions in the N-terminal globular domain would affect the assembly of the 12 arm oligomers into lattices. And indeed when cells overexpressing a deletion mutant involving a deletion in the head and coiled-coil domains were examined (Gueth-Hallonet *et al.*, 1998), no lattices were found. Taken together, the following roles can be assigned to the two end domains of NuMA during oligomerization. The C-terminal domain promotes assembly of NuMA dimers into higher order oligomers and the N-terminal domain controls the assembly of oligomers into lattices.

A role for NuMA as a scaffold protein in normal cells?

That NuMA might play a critical role in normal nuclear structure is suggested by two findings. First, NuMA interacts with MARs *in vitro* (Luderus *et al.*, 1994). Secondly, during apoptosis NuMA is proteolysed from a 238 kDa form to a 180–200 kDa form (Hsu and Yeh, 1996; Weaver *et al.*, 1996). We have suggested that the cleavage site leading to the stable fragment occurs between residues 1701 and 1725 (Gueth-Hallonet *et al.*, 1997). Examination of the models in Figure 7 suggests that cleavage of NuMA in this region, i.e. at the border between the coiled-coil and the tail regions, would cause the lattice to collapse. Thus, if normal cells have lattices that are built from NuMA, cleavage of NuMA might result on the one hand in the observed redistribution of DNA and NuMA and on the other hand cause the dramatic rearrangements of nuclear constituents seen during apoptosis. In addition, it has been suggested that NuMA may be involved in defining the nuclear shape in interphase cells and that the absence or degradation of NuMA may allow the cell to modulate the nuclear architecture to adapt to specific functions upon differentiation (Merdes and Cleveland, 1998).

Untransfected HeLa cells have, on average, 2×10^5 molecules NuMA per nucleus, which is some 40-fold less than the amount of NuMA seen in cells overexpressing the FL NuMA construct. Thus, lattices built from NuMA in normal cells cannot fill the nucleus and must therefore be spatially restricted. One way to reconcile the dotted pattern seen in HeLa cell nuclei with NuMA antibodies that recognize a defined epitope close to the C terminus of NuMA would be to imagine that NuMA assembles into many 'minilattices', each of which would be built using the principles elucidated for lattices in transfected cells. Minilattices could contain different numbers of NuMA molecules under different conditions, thus allowing rapid and dynamic changes in the size of NuMA aggregates in response to changes in the nuclear or cellular environment. Immunoelectron microscopy using gold-labelled NuMA antibodies has not shown lattices in normal cells, but because such lattices would be very much smaller and would not necessarily be interconnected, they may not survive the extraction and fixation steps used to reveal the lattices in transfected cells (Gueth-Hallonet *et al.*, 1998).

In summary, we have shown that bacterially expressed recombinant NuMA can self assemble *in vitro* under physiological salt conditions into a novel higher order structure, the multiarm oligomer. Computer modelling suggests that these multiarm oligomers could be the structural unit from which the lattices of NuMA seen by electron microscopy in nuclei of cells overexpressing NuMA are built. These lattices allow very close packing of NuMA into the nuclei and may be a prototype for the arrangement of NuMA or of other nuclear scaffold molecules in the normal interphase cell.

Materials and methods

Recombinant fragments of NuMA and FL NuMA

The λ phage isolates λ1 and λ2 from a HeLa cell cDNA library in the λ ZAP II vector (Harborth *et al.*, 1995) were used as templates for PCR amplification of the constructs λ1a (corresponding to amino acid residues

1–851) and λ2a (corresponding to residues 670–2115). PCR products were cloned in-frame into unique cloning sites of the pRSET A expression vector (Invitrogen, San Diego, CA). This expression vector contains a T7 promoter and a N-terminal His-tag plus adjacent T7 tag. In addition, the subfragments corresponding to the α-helical portion of NuMA (λ1c corresponding to residues 216–851 and λ2b corresponding to residues 670–1700) were amplified and cloned into the pRSETA vector.

Tailless and headless fragments and the FL construct were constructed from the overlapping clones λ1a or λ1c and λ2a or λ2b by digestion at the unique Bst EII site, occurring between the codons for amino acid positions 712 and 713. These constructs were designated according to the different portions of the tripartite secondary structure they contain, i.e. HCC (head and coiled-coil region, residues 1–1700, from λ1a and λ2b), CCT (coiled-coil region and tail, residues 216–2115, from λ1c and λ2a) and HCCT (head and coiled-coil region and tail equivalent to full length, residues 1–2115, from λ1a and λ2a). In addition, a further construct, HCCt, was made. It has the head and coiled-coil region plus the first part of the tail portion and corresponds to residues 1–2003.

Expression of recombinant polypeptides

Overexpression of the recombinant fusion proteins was as described (Harborth *et al.*, 1995). SOB medium (Invitrogen) (2 ml) containing 50 μg/ml of ampicillin was inoculated with a single recombinant *E.coli* JM109 colony that contained the appropriate plasmid. The culture was incubated overnight at 37°C with shaking and 0.8 ml was used to inoculate 200 ml SOB medium containing 50 μg/ml of ampicillin. The culture was grown at 37°C with shaking until it reached an optical density at 600 nm of 0.3. Expression was initiated by adding IPTG to a concentration of 1 mM. One hour later, cells were infected with M13/T7 phage at a multiplicity of infection of 5 plaque-forming units/cell. After a further 4 h, cells were harvested by centrifugation (4000 *g* for 20 min).

Purification of soluble recombinant polypeptides

Cells harvested from a 200 ml culture were suspended in 10 ml lysis buffer A (50 mM potassium phosphate pH 7.9, 500 mM KCl, 10 mM 2-mercaptoethanol, 1 mM PMSF, 0.2% Tween 20) and sonicated. The lysate was clarified by centrifugation at 10 000 *g* for 15 min. The recombinant fragment λ1a was soluble and was enriched by metal chelate affinity chromatography. The supernatant was applied to a Ni-NTA–agarose column (Qiagen, Hilden, Germany). The column was washed with buffer A and then with buffer B (identical to buffer A, except pH 6.0 and 20 mM imidazole). The recombinant protein was eluted with 500 mM imidazole in buffer B. The λ1a fragment was further purified by gel filtration on a Superdex 200 column (Pharmacia, Sweden).

Purification of insoluble recombinant NuMA proteins

All constructs other than λ1a were insoluble in lysis buffer and were purified as follows: the pellet was treated with urea buffer B (8 M urea, 20 mM Tris–HCl pH 7.9, 500 mM NaCl, 10 mM 2-mercaptoethanol) and then sonicated. After centrifugation, the supernatant was subjected to gel filtration in the presence of 8 M urea on a TSK G6000PW column (internal diameter 21.5 mm, length 60 cm, Toso Haas, Montgomeryville, PA) in buffer C [8 M urea, 20 mM Tris pH 7.2, 1 mM dithiothreitol (DTT), 2 mM EGTA]. Early fractions that contained the expressed fragments as assayed by SDS–PAGE, were pooled and subjected to anion exchange chromatography on Mono Q PC 1.6/5 (Pharmacia) in buffer C. Proteins were eluted in buffer C using a 0–0.9 M NaCl gradient. Integrity of the NuMA proteins was monitored by SDS–PAGE followed by immunoblotting with the NuMA monoclonal antibodies SPN3 or SPN7 (Kallajoki *et al.*, 1991).

Electron microscopy

The recombinant protein λ2a, purified by Mono-Q chromatography, was dialysed against 20 mM Tris–HCl pH 7.2, 20 mM NaCl, 1 mM DTT for at least 3 h at room temperature. Protein aliquots (50 μl) were placed on a nitrocellulose filter (0.025 μm, Millipore) floating on 50 ml buffer. The FL NuMA protein was renatured by dialysis against 20 mM Tris–HCl, pH 7.2, with 1 mM DTT, 1 mM EGTA and different salt concentrations of 150 mM NaCl (physiological salt), 20 mM NaCl (low salt) or 500 mM NaCl (high salt) for 3 h at room temperature. The recombinant fragments CCT, HCCt, and HCC as well as the HCCT full-length construct were eluted from Mono Q as described above and then dialysed against buffer D (25 mM Tris pH 7.55, 150 mM NaCl, 1 mM EGTA, 1 mM DTT, 1 mM PMSF and 1 mM $MgCl_2$).

For the equilibrium assay, the purified FL construct was dialysed against either physiological salt buffer (25 mM Tris, 1 mM EGTA, 1 mM DTT, 1 mM PMSF, 1 mM $MgCl_2$, 150 mM NaCl pH 7.6) or against high salt buffer (same composition except 500 mM NaCl and pH 7.1). Samples were dialysed for ~4 h at room temperature in parallel against either physiological or against high salt buffer. Other samples were dialysed first against high salt buffer and then against physiological salt buffer or vice versa.

Glycerol was added to the protein solutions to a final concentration of 50%. Protein solutions were then sprayed on to freshly cleaved mica flakes, which were subsequently dried under vacuum. The specimens were rotary shadowed with tantalum/tungsten or platinum at an angle of 5° or at 9° using a modified Balzers apparatus. They were then carbon shadowed at 90°. Replicas were floated off onto a surface of distilled water and collected on copper grids (400 mesh, TAAB, Munich, Germany).

Cell cuture and transfection

Electron microscopy of cells overexpressing the particular NuMA constructs shown in Figure 6 used HeLa SS6 cells grown as monolayers on glass coverslips. Cells were transiently transfected and 42 h later were extracted with microtubule stabilizing buffer (4 M glycerol, 100 mM PIPES pH 6.8, 1 mM EGTA, 5 mM $MgCl_2$, 0.5% Triton X-100) for ~3 min at room temperature and then fixed with glutaraldehyde and processed for electron microscopy (for details see Gueth-Hallonet *et al.*, 1998).

SDS gel electrophoresis and immunoblotting

SDS–PAGE was performed in 0.5 mm thick slab gels containing 10 or 5% acrylamide. For immunoblotting, polypeptides separated by SDS–PAGE were transferred electrophoretically onto nitrocellulose membranes. The transfer buffer contained 25 mM Tris, 190 mM glycine, 0.01% SDS and 20% methanol. The nitrocellulose strips were stained reversibly with Ponceau S. Blocking of the nitrocellulose membrane and subsequent immunological detection was as described previously (Harborth *et al.*, 1995). Peroxidase-conjugated second antibodies were detected with 4-chloronaphthol.

Acknowledgements

We thank Jürgen Schünemann and Heinz-Jürgen Dehne for expert technical assistance, and Martin Strahm for help with computer programming to generate the models.

References

Compton,D.A. and Cleveland,D.W. (1993) NuMA is required for the proper completion of mitosis. *J. Cell Biol.*, **120**, 947–957.

Compton,D.A. and Luo,C. (1995) Mutation of the predicted p34-cdc2 phosphorylation sites in NuMA impair the assembly of the mitotic spindle and block mitosis. *J. Cell Sci.*, **108**, 621–633.

Compton,D.A., Szilak,I. and Cleveland,D.W. (1992) Primary structure of NuMA an intranuclear protein that defines a novel pathway for segregation of proteins at mitosis. *J. Cell Biol.*, **116**, 1395–1408.

Gaglio,T., Saredi,A. and Compton,D.A. (1995) NuMA is required for the organization of microtubules into aster-like mitotic arrays. *J. Cell Biol.*, **131**, 693–708.

Gaglio,T., Saredi,A., Bingham,J.B., Hasbani,M.J., Gill,S.R., Schroer,T.A. and Compton,D.A. (1996) Opposing motor activities are required for the organization of the mammalian mitotic spindle pole. *J. Cell Biol.*, **135**, 399–414.

Gueth-Hallonet,C., Weber,K. and Osborn,M. (1996) NuMA: A bipartite nuclear location signal and other functional properties of the tail domain. *Exp. Cell Res.*, **225**, 207–218.

Gueth-Hallonet,C., Weber,K. and Osborn,M. (1997) Cleavage of the nuclear matrix protein NuMA during apoptosis. *Exp. Cell Res.*, **233**, 21–24.

Gueth-Hallonet,C., Wang,J., Harborth,J., Weber,K. and Osborn,N. (1998) Induction of a regular nuclear lattice by overexpression of NuMA. *Exp. Cell Res.*, **243**, 434–452.

Harborth,J., Weber,K. and Osborn,M. (1995) Epitope mapping and direct visualization of the parallel, in-register arrangement of the double-stranded coiled-coil in the NuMA protein. *EMBO J.*, **14**, 2447–2460.

Hsu,H.L. and Yeh,N.H. (1996) Dynamic changes of NuMA during the cell cycle and possible appearance of a truncated form of NuMA during apoptosis. *J. Cell Sci.*, **109**, 277–288.

Kallajoki,M., Weber,K. and Osborn,M. (1991) A 210 kDa nuclear matrix protein is a functional part of the mitotic spindle a microinjection study using SPN monoclonal antibodies. *EMBO J.*, **10**, 3351–3362.

Kallajoki,M., Harborth,J., Weber,K. and Osborn,M. (1993) Microinjection of a monoclonal antibody against SPN antigen now identified by peptide sequences as the NuMA protein induces micronuclei in PtK2 cells. *J. Cell Sci.*, **104**, 139–150.

Luderus,M.E., den Blaauwen,J.L., de Smit,O.J., Compton,D.A. and van Driel,R. (1994) Binding of matrix attachment regions to lamin polymers involves single-stranded regions and the minor groove. *Mol. Cell. Biol.*, **14**, 6297–6305.

Lydersen,B.K. and Pettijohn,D.E. (1980) Human-specific nuclear protein that associates with the polar region of the mitotic apparatus: distribution in a human/hamster hybrid cell. *Cell*, **22**, 489–499.

Merdes,A. and Cleveland,D.W. (1998) The role of NuMA in the interphase nucleus. *J. Cell Sci.*, **111**, 71–79.

Merdes,A., Ramyar,K., Vechio,J.D. and Cleveland,D.W. (1996) A complex of NuMA and cytoplasmic dynein is essential for mitotic spindle assembly. *Cell*, **87**, 447–458.

Parry,D.A.D. (1994) NuMA-centrophilin: Sequence analysis of the coiled-coil rod domain. *Biophys. J.*, **67**, 1203–1206.

Saredi,A., Howard,L. and Compton,D.A. (1996) NuMA assembles into an extensive filamentous structure when expressed in the cell cytoplasm. *J. Cell Sci.*, **109**, 619–630.

Saredi,A., Howard,L. and Compton,D.A. (1997) Phosphorylation regulates the assembly of NuMA in a mammalian mitotic extract. *J. Cell Sci.*, **110**, 1287–1297.

Sparks,C.A., Fey,E.G., Vidair,C.A. and Doxsey,S.J. (1995) Phosphorylation of NuMA occurs during nuclear breakdown and not mitotic spindle assembly. *J. Cell Sci.*, **108**, 3389–3396.

Weaver,V.M., Carson,C.E., Walker,P.R., Chaly,N., Lach,B., Raymond,Y., Brown,D.L. and Sikorska,M. (1996) Degradation of nuclear matrix and DNA cleavage in apoptotic thymocytes. *J. Cell Sci.*, **109**, 45–56.

Yang,C.H. and Snyder,M. (1992) The nuclear-mitotic apparatus protein is important in the establishment and maintenance of the bipolar mitotic spindle apparatus. *Mol. Biol. Cell*, **3**, 1259–1267.

Yang,C.H., Lambie,E.J. and Snyder,M. (1992) NuMA an unusually long coiled-coil related protein in the mammalian nucleus. *J. Cell Biol.*, **116**, 1303–1317.

Received November 27, 1998; revised and accepted January 20, 1999